RSC Advances

ROYAL SOCIETY OF CHEMISTRY

www.rsc.org/advances

Table of Contents

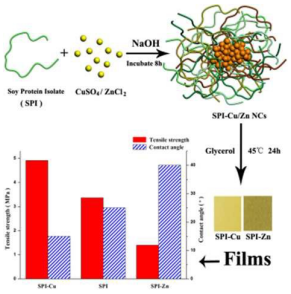

Special bio-films from SPI regulated by endogenous Cu and Zn nanoclusters perform excellent hydrophobicity and flexibility.

Journal Name

ARTICLE

Endogenous Cu and Zn nanoclusters-regulated soy protein isolate films: excellent hydrophobicity and flexibility

Received 00th January 20xx,
Accepted 00th January 20xx

DOI: 10.1039/x0xx00000x

www.rsc.org/

Kuang Li,† Hui Chen,† Ying Li, Jianzhang Li* and Jing He*

Water-soluble Cu nanoclusters (NCs) and Zn NCs capped with a vegetable protein, soy protein isolate (SPI), are designed and synthesized for regulation of the rigidity and flexibility of bio-films. The special bio-films from SPI modified by Cu NCs exhibit better mechanical property, and those modified with Zn NCs show better hydrophobic property. UV-vis absorption spectra demonstrated that Cu NCs and Zn NCs have formed, and Fourier transform infrared spectroscopy revealed that there was no change in the basic structure of protein, but the SPI molecule chains and functional groups might be influenced, which made the cross-linking density increase. X-ray photoelectron spectroscopy suggested Cu and Zn were in the zero-valent state. X-ray diffraction patterns of SPI films indicated that metal nanoclusters changed the conformation of SPI from compact to unfolded. Water vapor permeability, oxygen permeability and nitrogen permeability of these metal nanoclusters-modified films have been improved, and these films are proven safe enough to be used in contact with food.

1. Introduction

In recent years, with the wide use of petroleum-based materials around the world, their negative impact of wastes from disposable plastic items has risen and become a serious issue.[1,2] The use of biopolymer-based films can solve the waste disposal problem to a certain extent.[3] Compared with conventional petroleum-based polymers, biopolymers offer favorable environmental advantages of recyclability and reutilization.[4]

Among other biopolymers, soy protein has been impressively used for the development of biodegradable films due to its relative abundance and good film-forming ability.[5] Soy protein is a kind of agricultural processing by-product of the soybean oil industry, most of them (90%) are globulins, which can be fractionated into 2S, 7S, 11S and 15S according to their sedimentation coefficients. 7S and 11S are the main fractions being about 37% and 31% of the total extractable protein and have the capacity of polymerization.[6] However, soy protein plastics have poor mechanical properties and high sensitivity to moisture, which limit their applications. Therefore, efforts should be made to modify their brittleness and to improve their water resistance.

The development of new nanocomposites has excited a lot of interest as it may improve the polymer properties and extend their application field.[7,8] Functional nanomaterials is becoming increasingly widespread in consumer technologies.[9,10] Synthesis of nanocrystals-crystalline particles ranging in size from 1 to 100 nm has been intensively pursued, not only for their fundamental scientific interest, but also for their many technological applications in different fields.[11,12] The potential application of nanoparticles, such as optoelectronics, catalysis, coatings, nanostructure fabrication and sensors has made a great impact in the world of technology.[13-16] Metal nanoclusters (NCs) defined as isolated particles less than 2 nm in size with several to a hundred atoms, which are ultrafine particles of nanometer dimensions located in the transition region between atoms and bulk solids.[17,18] This particle size is further reduced and approaches the Fermi wavelength of electrons, the continuous density of states breaks up into discrete energy levels leading to the observation of dramatically different optical, electrical and chemical properties compared to nanoparticles.[19-21] Metal nanoclusters exhibited unique physical and chemical properties, as well as had practical applications in various areas.[22-25] Compared with other noble metals, Cu NCs and Zn NCs are attracting a wealth of attention in many areas of nanotechnology.[26] Due to their superior properties, such as low toxicity, good biocompatibility and multifunctional surface chemistry, they have already been recognized as potential catalytic agents.[27-31] However, the synthesis of Cu NCs and Zn NCs requires strict conditions, and the application of them in new fields is still in development.

Soy protein isolate (SPI), which contains more than 90% protein and consists of 18 different amino acids, is an abundant vegetable protein with good biodegradability and film-forming ability.[32] In this work, we designed and synthesized a water-soluble Cu NCs and Zn NCs with soy protein as template for the first time, and a new application of endogenous metal nanoclusters in bionanocomposite films

MOE Key Laboratory of Wooden Material Science and Application, Beijing Key Laboratory of Wood Science and Engineering, College of Materials Science and Technology, Beijing Forestry University, Beijing 100083, China. E-mail: lijzh@bjfu.edu.cn, Hejing2008@sina.com; Phone/Fax: +86-10-62338083
† These authors contributed equally.

based on SPI was investigated. The improved mechanical property and relatively low moisture sensitivity of SPI films after modification by endogenous metal nanoclusters showed wide potential applications in bearing and flexible packaging materials.

2. Experimental

2.1 Materials

SPI with protein content of 95% was purchased from Yuwang Ecological Food Industry Co., Ltd. (Shandong province, China). Copper sulphate anhydrous and zinc chloride were provided by Beijing Chemical Works (BeiJing, China). Glycerol (99% purity) was obtained from Beijing Chemical Reagents. Sodium hydroxide of analytical grade was provided by Beijing Chemical Reagents. Deionized water was used for the preparation of all solutions.

2.2 Apparatus

High resolution TEM images were recorded on a FEI Tecnai G2 F20 transmission electron microscopy at 200 kV of acceleration voltage (FEI, Oregon, USA). Absorption spectra were collected using a TU-1901 UV-Vis spectrophotometer (Beijing Purkinje General, Beijing, China). Attenuated total reflectance-Fourier transformed infrared (ATR-FTIR) spectra were carried out on a Nicolet 6700 spectrometer (Thermo Scientific, Pittsburgh, USA), in the range of 4000-650 cm^{-1}, using an ATR accessory with a diamond crystal. A total of 32 scans were performed at 4 cm^{-1} resolution. The X-ray photoelectron spectroscopy (XPS) was carried out on a PHI Quantera SXM spectrometer with an Al Kα X-ray source (ULVAC-PHI, Chigasaki, Japan). X-ray diffraction (XRD) was performed on a D8 advance diffractometer (Bruker, U.S.A) equipped with a Cu Kα radiation source (λ=0.154 nm). The diffraction data were collected 2θ from 5° to 60° in a fixed time mode with a step interval of 0.02°. Surface hydrophobicity was assessed by contact angle using an OCA20 contact angle meter (Dataphysics Co., Ltd, Germany). A film sample (20 mm × 80 mm) was placed on a movable carrier and levelled horizontally. 3 μL drop of distilled water was dropped on the film surface using a microsyringe. Five replicates were done for each film. Tensile properties were determined using a tensile testing machine (WDW3020, China) at a speed of 10 mm/min at room temperature. The average of five replicates was calculated as tensile strength (TS), Young's modulus (E) and elongation at break (EB) values. The oxygen permeability and nitrogen permeability of these films were measured using M-3 gas permeation analyzer (Toyosk, Japan) in China Packaging Research & Test Center (Tianjin, China). The metal content was measured on a Leeman Prodigy inductively coupled plasma-optical emission spectroscopy (Prodigy XP, Hudson, USA).

2.3 Preparation of SPI-Cu NCs and SPI-Zn NCs films

SPI film-forming solutions were prepared by dissolving 4.0 g SPI in constantly magnetically stirred distilled water (80 mL). 8 mL 20 mmol/L $CuSO_4$ or $ZnCl_2$ solution was added to the SPI solution. The mixing solution was stirred at room temperature for 10 min, then NaOH solution was introduced to adjust pH about 12. The mixture was heated with stirring at 75 ^{o}C for 8 h for the preparation of metal nanoclusters. Finally, 2.0 g glycerol (50% of SPI, w/w) was added to these solutions. After heating at 85 ^{o}C for 30 min in a constant temperature water bath, solutions were subsequently poured onto leveled polystyrene plates. Film thickness was controlled by casting the same amount (40 g) of the solution per plate. The castings were dried in drying oven at 45 ^{o}C for at least 24 h before testing. Films were named as SPI-X, where X corresponds to the metal added.

2.4 Water vapor permeability (WVP)

Water vapor permeability was measured using water vapor permeability tester (TSY-T1, Jinan, China) according to the ASTM E96-01 method (ASTM, 2001b). The specimen with the diameter of 10 cm was mounted to the dish and placed in the controlled chamber at 25 ^{o}C and 50 % relative humidity. Final measurement was done after incubation for 11 h. Five replicates were tested for each specimen and the WVP was calculated by eqn(1).

$$WVP = WVTRx / [P_0 (RH_1 - RH_2)] \quad (1)$$

Where WVTR was the measured water vapor transmission rate (g/m^2 h) through a film sample, x is the film thickness (mm); P_0 is the vapor pressure of pure water (25 ^{o}C, 3.159 kPa); and (RH_1 - RH_2) is the relative humidity gradient used in the experiment.

3. Results and discussion

3.1 Characterization of SPI-based Cu NCs and Zn NCs

The size distribution of Cu NCs and Zn NCs based on SPI was characterized by high resolution transmission electron microscopy (HRTEM). HRTEM images of the synthesized Cu NCs and Zn NCs were shown in Fig. 1. All metal nanoclusters were grown in the SPI substrate. Cu NCs dispersed uniformly in solution (Fig. 1a), and the average size of single nanocluster was about 5 nm (Fig. 1b). However, the preparation requirement of Zn NCs showed stricter, and the size of Zn NCs was less than 10 nm, which was larger than that of Cu NCs (Fig. 1c and 1d).

To confirm that Cu NCs and Zn NCs were prepared successfully by the template of SPI, UV-vis absorption spectra were collected. Fig. 2a showed the UV-vis absorption spectra of SPI, SPI-Cu NCs and SPI-Zn NCs. The pure SPI has a broad absorption spectrum at 280 nm. An obvious red shift was observed from the absorption peak of SPI-Cu NCs or SPI-Zn NCs. It demonstrated that new substance such as Cu NCs and Zn NCs has been formed.[33]

ATR-FTIR spectra were performed to investigate the change of functional groups in SPI film modified with Cu NCs and Zn NCs (Fig. 2b). All SPI films exhibited three characteristic amide bands, amide I at 1632 cm^{-1} (C=O stretching), amide II at 1538 cm^{-1} (N-H bending) and amide III at 1237 cm^{-1} (C=N

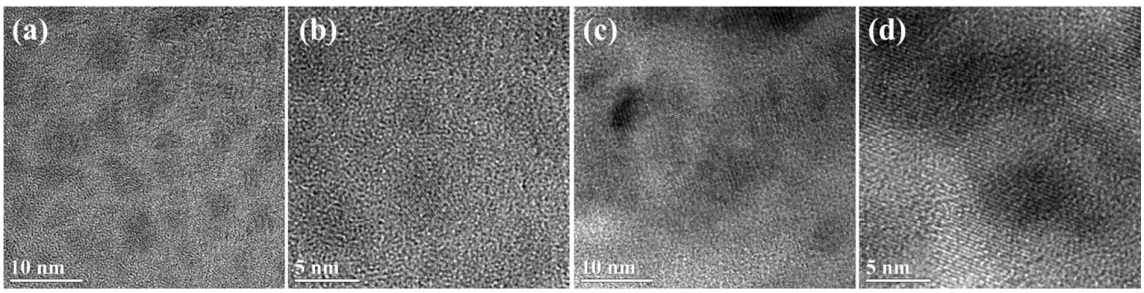

Fig. 1 HRTEM images of Cu NCs (a, b) and Zn NCs (c,d) capped with soy protein isolate.

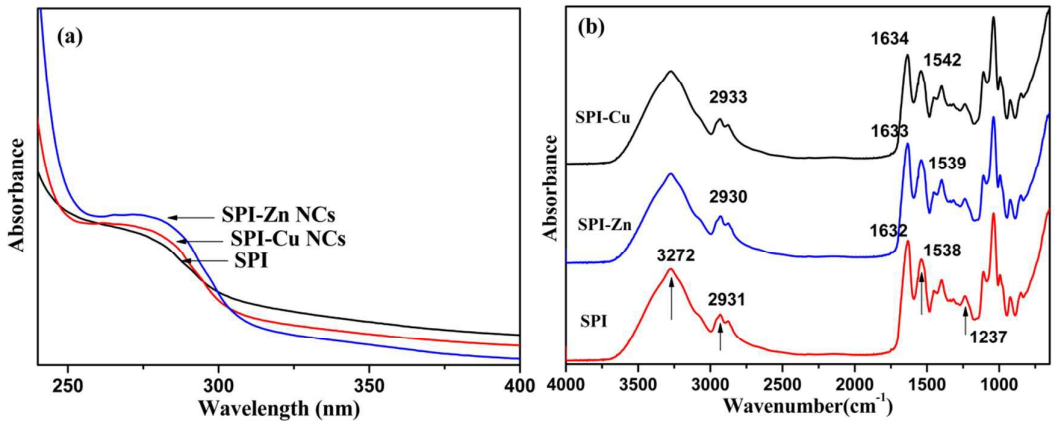

Fig. 2 UV-vis absorption spectra of SPI, SPI-Cu NCs and SPI-Zn NCs (a), and ATR-FTIR spectra of SPI films untreated and treated with Cu NCs and Zn NCs, respectively (b).

stretching), respectively.[34] Amide I and II of SPI films treated by metal nanoclusters shifted to higher wavenumbers. This change suggested that hydrogen bonding existed between SPI and metal nanoclusters, and the metal nanoclusters made SPI structure more unfolded and loose. Moreover, metal nanoclusters induced a slight reduction in the intensity of the amide II band, which is generally related with changes in hydrogen bonding, confirming that metal nanoclusters might act by interacting with protein chains and reducing the bindings between the chains. Meanwhile, Amide I and II of SPI-Cu NCs film shifted to higher wavenumbers than that of SPI-Zn NCs film, which indicated that SPI-Cu NCs film exposed more polar groups. So we draw a conclusion that Cu NCs and Zn NCs cannot change the basic structure of protein, but more likely to influence the patterns of SPI molecule chains and the distribution of functional groups, resulting in increasing the cross-linking density and improving mechanical properties of films.

3.2 X-ray photoelectron spectroscopy analysis

XPS was carried out to analysis the oxidation state of copper and zinc in the SPI-Cu NCs and SPI-Zn NCs films. All expected elements were shown in the survey spectrum (Fig. 3a). Compared with the SPI film, two peaks of Cu and Zn could be observed in the SPI-Cu NCs film and SPI-Zn NCs film, respectively. The binding energy of Cu2p showed at 932.3 eV and 952.0 eV, demonstrated that Cu was in the zero-valent state (Fig. 3b). The peak of Zn2p was located at 1021.7 eV and 1044.81 eV, suggesting the presence of Zn (0) in the film (Fig. 3c).[35]

3.3 X-ray diffraction patterns and contact angles analysis

X-ray diffraction experiment was carried out to investigate the change in the structure of the films prepared with different metal nanoclusters. Fig. 4a displayed the XRD patterns of SPI films untreated and treated with different kinds of metal nanoclusters. The two diffraction peaks of control film at 2θ of about 10° and 20° were the strong characteristic peaks of SPI, which were agreed with the reports.[36] It could be observed that the peak at 2θ of about 9° diminished and disappeared when films modified by metal nanoclusters, indicating that metal nanoclusters made the conformation of SPI changed and transformed the compact structure of SPI to the partially unfolded.

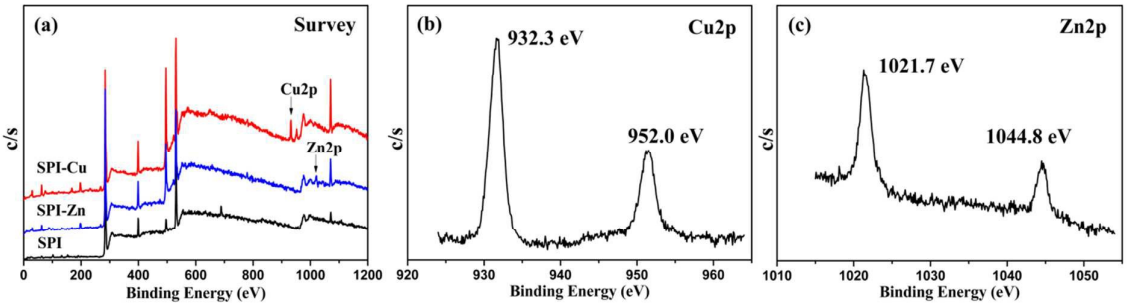

Fig. 3 XPS spectra of SPI-based films. Survey of SPI films untreated and treated with Cu NCs and Zn NCs (a), Cu2p of SPI-Cu NCs (b), and Zn2p of SPI-Zn NCs (c).

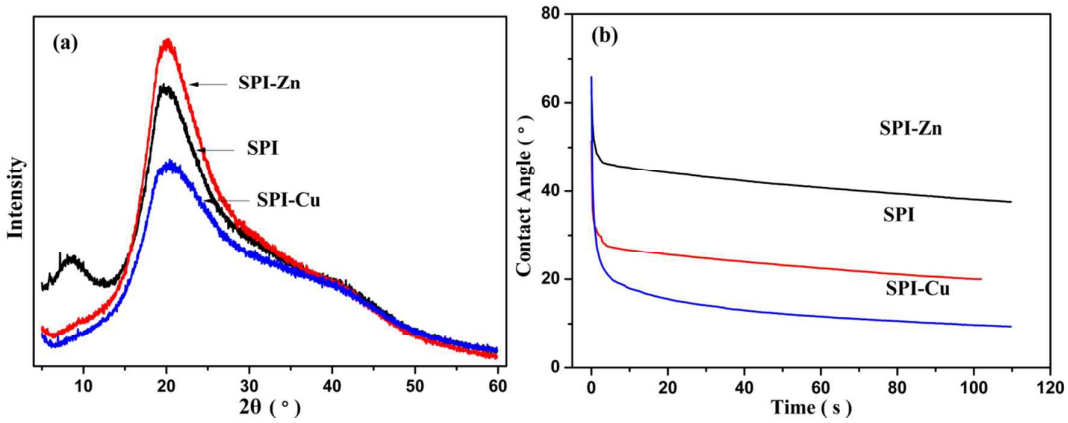

Fig. 4 XRD patterns (a) and contact angles (b) of SPI films untreated and treated with Cu NCs and Zn NCs, respectively.

Thus SPI could expose more active groups and prompt reactions between functional groups. Furthermore, the intensity of the peak at 2θ value of about 20° of SPI-Cu NCs films lowered a lot compared to SPI films, indicating the crosslinking between Cu NCs and SPI changed the conformation of the protein molecules, reducing the regular arrangement of molecular chains and making the crystalline structure of SPI partially collapsed. However, SPI-Zn NCs films exhibited a higher intensity of the peak at 2θ about 20°. It indicated that a higher degree of compact structure of SPI was produced by the protein-metal nanoclusters interactions, causing the poorer tensile strength of films.

The contact angles of films were shown in Fig. 4b, which were indicators of surface hydrophilicity. As can be seen, SPI-Zn NCs films showed the highest contact angles. This behaviour indicated that SPI-Zn NCs interactions could result in a higher exposure of hydrophobic groups of SPI, thus increasing hydrophobicity of the films.[37] However, the SPI-Cu NCs film exhibited a low water contact angle, indicating a highly hydrophilic and wettable surface, which was due to the higher content of polar groups on the film surface.

3.4 Physical and mechanical properties

The effects of metal nanoclusters on mechanical properties of SPI films were shown in Table 1. With the modification of Cu NCs, the tensile strength (TS) and Young's modulus (E) of SPI film increased, while elongation at break (EB) value decreased. This may be attributed to the strong interactions between SPI and Cu NCs. The unfolded and loose structure of SPI modified by Cu NCs was also evidenced by the decrease of crystallinity in XRD results. This kind of structure improved interactions among protein molecules, because they were brought closer together and the contact area among them was increased, which in turn will bring about higher molecular entanglements and improve the mechanical properties of SPI.[38]

Table 1 Tensile strength, Young's modulus and elongation at break of SPI films untreated and treated with Cu NCs and Zn NCs.

Samples	TS (MPa)	E (MPa)	EB (%)
SPI	3.36	60.25	192.55
SPI-Cu NCs	4.91	104.25	131.72
SPI-Zn NCs	1.40	6.35	304.05

The TS and E of SPI film decreased with the treatment of Zn NCs, indicating the films were greatly softened, whereas the values of EB significantly increased from 192.55% to 304.05%. This could be ascribed to the fact that the interactions between SPI and Zn NCs, which had a plasticizing effect on protein matrix and improved the flexibility of the material. These properties of SPI film were mainly due to the binding capacity difference of Cu NCs and Zn NCs with –SH group in SPI.[39,40]

Table 2 Water vapor permeability, oxygen permeability and nitrogen permeability of SPI films untreated and treated with Cu NCs and Zn NCs.

Sample	WVP (g mm/m^2 h kPa)	O_2 (cm^3/m^2 24h 0.1MPa)	N_2 (cm^3/m^2 24h 0.1MPa)
SPI	3.200	12.42	3.08
SPI-Cu NCs	2.563	3.93	1.03
SPI-Zn NCs	2.837	5.42	2.20

3.5 Water vapor permeability, oxygen permeability and nitrogen permeability test

High water vapor permeability, oxygen permeability and nitrogen permeability of the film are not desirable with respect to its usage performance.[41] Table 2 showed the values of water vapor permeability, oxygen permeability and nitrogen permeability of these SPI-based films. The value of O_2 permeability of SPI-Cu NCs and SPI-Zn NCs films was 3.93 and 5.42, respectively. They were much lower than that of SPI film, which was 12.42. From Table 2, it also can be observed that these values of water vapor permeability and N_2 permeability of SPI-Cu NCs and SPI-Zn NCs films were all lower than those of SPI film. This suggested that the treatment of metal nanoclusters could improve the water vapour, oxygen and nitrogen barrier ability of SPI films. It was favorable for food packaging materials.

3.6 Release test of Cu and Zn from the SPI-based films

5.0 g SPI-Cu NCs film or SPI-Zn NCs film was dissolved in 50 mL water and heated for 2 hours at 100 °C. The release of Cu and Zn was measured on a Leeman ICP spectroscopy. Results indicated that the concentration of Cu and Zn released from the films was 2.81 ppm and 16.62 ppm, respectively (Table 3). It's safe when they were put in contact with food.

Table 3 Release content of Cu and Zn from the SPI-Cu NCs film and SPI-Zn NCs film

SPI-Cu NCs film	Cu (324.754 nm) (ppm)	SPI-Zn NCs film	Zn (213.856 nm) (ppm)
Sample 1	2.8027	Sample 1	16.6468
Sample 2	2.8135	Sample 2	16.6020
Sample 3	2.8307	Sample 3	16.6485
Sample 4	2.8153	Sample 4	16.6063
Sample 5	2.8081	Sample 5	16.6244
Sample 6	2.8230	Sample 6	16.6274
Average	2.8156±0.01	Average	16.6259±0.02

Conclusions

In conclusion, a simple and convenient method for the synthesis of water-soluble Cu NCs and Zn NCs capped with a vegetable protein has been developed. The SPI films treated with endogenous Cu NCs showed better mechanical properties and that modified by endogenous Zn NCs performed higher flexibility and hydrophobicity. They all exhibited good water vapor, oxygen and nitrogen barrier ability. These SPI films modified with metal nanoclusters have the potential to be used as packaging materials in food, pharmaceutical and cosmetics fields with the advantages of renewable and biodegradable.

Acknowledgements

This work was supported by Beijing Natural Science Foundation (No. 2151003) and China Postdoctoral Science Foundation (No. 2014M560052).

Notes and references

1 L. Bueno, G. N. Meloni, S. M. Reddy and T. R. L. C. Paixão, *RSC Adv*., 2015, **5**, 20148-20154.
2 T. Garrido, A. Etxabide, M. Peñalba, K de la. Caba and P. Guerrero, *Mater. Lett.,* 2013, **105**, 110-112.
3 S. Raut, R. Chib, R. Rich, D. Shumilov, Z. Gryczynskia and I. Gryczynski, *Nanoscale*, 2013, **5**, 3441-3446.
4 A. Shaabani, Z. Hezarkhani and E. Badali, *RSC Adv*., 2015, **5**, 61759-61767.
5 Y. A. Arfat, S. Benjakul, T. Prodpran and K. Osako, *Food Hydrocolloids,* 2014, **39**, 58-67.
6 S. Sett, M. W. Lee, M. Weith, B. Pourdeyhimi and A. L. Yarin, *J. Mater. Chem. B*, 2015, **3**, 2147-2162.
7 R. Takemori, G. Ito, M. Tanaka and H. Kawakami, *RSC Adv*., 2014, **4**, 20005-20009.
8 Y. Lu and W. Chen, Chem. *Soc. Rev*., 2012, **41**, 3594-3623.
9 R. J. Moon, A. Martini, J. Nairn, J. Simonsen and J. Youngblood, *Chem. Soc. Rev*., 2011, **40**, 3941-3994.
10 M. Hyotanishi, Y. Isomura, H. Yamamoto, H. Kawasaki and Y. Obora, *Chem. Commun*., 2011, **47**, 5750-5752.
11 H. W. Li, K. L. Ai and Y. Q. Wu, *Chem. Commun*., 2011, **47**, 9852-9854.
12 W. T. Wei, Y. Z. Lu, W. Chen and S. W. Chen, *J. Am. Chem. Soc*., 2011, **133**, 2060-2063.
13 M. X. Yu, C. Zhou, J. B. Liu, J. D. Hankins and J. Zheng, *J. Am. Chem. Soc.,* 2011, **133**, 11014-11017.
14 J. P. Xie, Y. G. Zheng and J. Y. Ying, *Chem. Commun*., 2010, **46**, 961-963.
15 J. Chen, J. Liu, Z. Fang and L. Zeng, *Chem. Commun*., 2012, **48**, 1057-1059.
16 X. P. Wang, B. C. Yin and B. C. Ye, *RSC. Adv*., 2013, **3**, 8333-8636.
17 L. Shang, S. Dong and G. U. Nienhaus, *Nano Today,* 2011, **6**, 401-418.
18 H. Xu and K. S. Suslick, *Adv. Mater.,* 2010, **22**, 1078-1082.
19 L. Shang and S. Dong, *Chem. Commun*., 2008, 1088-1090.
20 H. Zhang, X. Huang, L. Li, G. Zhang, I. Hussain, Z. Li and B. Tan, *Chem. Commun*., 2012, **48**, 567-569.
21 J. S. Shen, D. H. Li, Q. G. Cai and Y. B. Jiang, *J. Mater. Chem*., 2009, **19**, 6219-6224.
22 D. M. Chevrier, A. Chatt and P. Zhang, *J. Nanophotonics,* 2012, **6**, 064504.
23 B. D. Martin, J. Fontana, Z. Wang, J. Louis-Jean and S. A. Trammell, *Chem. Commun*., 2012, **48**, 10657-10659.
24 X. Huang, B. Li, H. Zhang, I. Hussain, L. Liang and B. Tan, *Nanoscale*, 2011, **3**, 1600-1607.
25 R. Gui and H. Jin, *Analyst*, 2013, **138**, 7197-7205.
26 R. Gui, J. Sun, X. Cao, Y. Wang and H. Jin, *RSC Adv*., 2014, **4**, 29083-29088.
27 J. P. Wilcoxon and B. L. Abrams, Chem. *Soc. Rev*., 2006, **35**, 1162-1194.
28 R. Niranjan, V. Chaudhary, I. Mulla and K. Vijayamohanan, *Sensor. Actuat. B-Chem.,* 2002, **85**, 26-32.
29 P. Wu and X. P. Yan, *Chem. Commun*., 2010, **46**, 7046-7048.

30 I. Diez and R. H. A. Ras, *Nanoscale*, 2011, **3**, 1963-1970.
31 H. Tian, G. Xu, B. Yang and G. Guo, *J. Food Eng.,* 2011, **107**, 21-26.
32 Z. Wang, X. X. Sun, Z. X. Lian, X. X. Wang, J. Zhou and Z. S. Ma, J. Food Eng., 2013, **114**, 183-191.
33 W. Gao, X. Wang, W. Xua and S. Xu, *Mat. Sci. Eng*., 2014, **42**, 333-340.
34 H. Tian, Y. Wang, L. Zhang, C. Quan and X. Zhang, *Ind. Crop. Prod.,* 2010, **32**, 13-20.
35 C. Wang, C. Wang, L. Xu, H. Cheng, Q. Lin and C. Zhang, *Nanoscale,* 2014, **6**, 1775-1781.
36 S. Y. Wang, B. B. Zhu, D. Z. Li, X. Z. Fu and L. Shi, *Mater. Lett.,* 2012, **83**, 42-45.
37 P. Guerrero, P. M. Stefani, R. A. Ruseckaite and K. de la Caba, *J. Food. Eng.,* 2011, **105**, 65-72.
38 P. Guerrero, I. Leceta, M. Peñalba and K de la. Caba, *Mater. Lett.,* 2014, **124**, 286-288.
39 W. Zheng, Z. Wang, J. van Tol, N. S. Dalal and G. F. Strouse, *Nano Lett.,* 2012, **12**, 3132-3137.
40 H. Chen, L. Lin, H. Li, J. Li and J.-M. Lin, *ACS Nano,* 2015, **9**, 2173-2183.
41 S. Kokoszka, F. Debeaufort, A. Hambleton, A. Lenart and A. Voilley, *Innov. Food Sci. Emerg*., 2010, **32**, 13-20.